



**HAL**  
open science

## Extreme in-plane upper critical magnetic fields of heavily doped quasi-two-dimensional transition metal dichalcogenides

P Samuely, P Szabó, J Kačmarčík, A Meerschaut, L Cario, A G M Jansen, Tristan Cren, M Kuzmiak, O Šofranko, T Samuely

### ► To cite this version:

P Samuely, P Szabó, J Kačmarčík, A Meerschaut, L Cario, et al.. Extreme in-plane upper critical magnetic fields of heavily doped quasi-two-dimensional transition metal dichalcogenides. *Physical Review B*, 2021, 104, 10.1103/physrevb.104.224507 . hal-03853829

**HAL Id: hal-03853829**











**<https://hal.science/hal-03853829v1>**

Submitted on 15 Nov 2022

**HAL** is a multi-disciplinary open access archive for the deposit and dissemination of scientific research documents, whether they are published or not. The documents may come from teaching and research institutions in France or abroad, or from public or private research centers.

L'archive ouverte pluridisciplinaire **HAL**, est destinée au dépôt et à la diffusion de documents scientifiques de niveau recherche, publiés ou non, émanant des établissements d'enseignement et de recherche français ou étrangers, des laboratoires publics ou privés.

## Extreme in-plane upper critical magnetic fields of heavily doped quasi-two-dimensional transition metal dichalcogenides

P. Samuely <sup>1,2,\*</sup>, P. Szabó <sup>1</sup>, J. Kačmarčík <sup>1</sup>, A. Meerschaut <sup>3</sup>, L. Cario <sup>3</sup>, A. G. M. Jansen <sup>4,5</sup>,  
T. Cren <sup>6</sup>, M. Kuzmiak <sup>1</sup>, O. Šofranko <sup>1,2</sup> and T. Samuely <sup>2</sup>

<sup>1</sup>Centre of Low Temperature Physics, Institute of Experimental Physics, Slovak Academy of Sciences, 04001 Košice, Slovakia

<sup>2</sup>Centre of Low Temperature Physics, Faculty of Science, P. J. Šafárik University, 04001 Košice, Slovakia

<sup>3</sup>Institut des Matériaux Jean Rouxel, Université de Nantes and CNRS-UMR 6502, Nantes 44322, France

<sup>4</sup>Université Grenoble Alpes, CEA, Grenoble INP, IRIG, PHELIQS, F-38000 Grenoble, France

<sup>5</sup>Laboratoire National des Champs Magnétiques Intenses (LNCMI-EMFL), CNRS, UGA, F-38042 Grenoble, France

<sup>6</sup>Institut des NanoSciences de Paris, Sorbonne Université and CNRS-UMR 7588, Paris 75005, France



(Received 8 July 2021; revised 9 November 2021; accepted 30 November 2021; published 20 December 2021)

Extreme in-plane upper critical magnetic fields  $B_{c2//ab}$  strongly violating the Pauli paramagnetic limit have been observed in the misfit layer  $(\text{LaSe})_{1.14}(\text{NbSe}_2)$  and  $(\text{LaSe})_{1.14}(\text{NbSe}_2)_2$  single crystals with  $T_c = 1.23$  and  $5.7$  K, respectively. The crystals show a two-dimensional to three-dimensional transition at temperatures slightly below  $T_c$  with an upturn in the temperature dependence of  $B_{c2//ab}$ , a temperature-dependent huge superconducting anisotropy and a cusplike behavior of the angular dependence of  $B_{c2}$ . Both misfits are characterized by a strong charge transfer from LaSe to NbSe<sub>2</sub>. As shown in our previous work,  $(\text{LaSe})_{1.14}(\text{NbSe}_2)_2$  is electronically equivalent to the highly doped NbSe<sub>2</sub> monolayers. Then, the strong upper critical field can be attributed to the Ising coupling recently discovered in atomically thin transition metal dichalcogenides with strong spin-orbit coupling and a lack of inversion symmetry. A very similar behavior is found in  $(\text{LaSe})_{1.14}(\text{NbSe}_2)$ , where the charge transfer is nominally twice as big, which could eventually lead to complete filling of the NbSe<sub>2</sub> conduction band and opening superconductivity in LaSe. Whatever the particular superconducting mechanism would be, a common denominator in both misfits is that they behave as a stack of almost decoupled superconducting atomic layers, proving that Ising superconductivity can also exist in bulk materials.

DOI: [10.1103/PhysRevB.104.224507](https://doi.org/10.1103/PhysRevB.104.224507)

Recently, a new type of superconducting interaction—the Ising pairing—was discovered in the atomically thin superconductors MoS<sub>2</sub> [1] and NbSe<sub>2</sub> [2]. The lack of crystal inversion symmetry in monolayer combined with strong spin-orbit coupling leads to an effective spin-orbit magnetic field. This fixes the electron spins out of plane (Ising) with opposite signs for the opposite momenta at  $K$  and  $K'$  of the hexagonal Brillouin zone. The locking of spin and momentum in the superconducting pairing hinders the spin pair-breaking leading to anomalously high in-plane upper critical fields violating the Pauli limit  $B_P$ . In NbSe<sub>2</sub> [2], the Zeeman spin splitting is realized at fields that exceed the superconducting condensation energy almost seven times. It was also shown that upon increasing the number of NbSe<sub>2</sub> atomic layers with the onset of interlayer coupling and the restoring of inversion symmetry, the in-plane critical field becomes smaller than  $B_P$ , calling into question the application of Ising superconductivity in bulk materials.

Here we show that nonconventional superconductivity is at play in a family of bulk compounds made of stacked NbSe<sub>2</sub> and LaSe layers. Our transport and ac calorimetry measurements down to millikelvin temperatures and in magnetic fields up to 30 T show that in both misfit layer

compounds— $(\text{LaSe})_{1.14}(\text{NbSe}_2)$  and  $(\text{LaSe})_{1.14}(\text{NbSe}_2)_2$ —the in-plane critical field  $B_{c2//ab}$  is overcoming the Pauli limiting  $B_P$  almost 10 and 5 times, respectively. The superconducting anisotropy  $\gamma = B_{c2//ab}/B_{c2//c}$  is very high and temperature-dependent. Moreover, the temperature dependence of  $B_{c2//ab}$  displays an upturn close to  $T_c$ , characteristic of a dimensional crossover in vortex matter from three-dimensional (3D) to two-dimensional (2D) upon lowering the temperature. The quasi-2D regime is manifested by a cusp in the angular dependence of  $B_{c2}$ .

Let us first focus on  $(\text{LaSe})_{1.14}(\text{NbSe}_2)_2$ , which is constituted of trilayers where one quasiquadratic ( $Q$ ) LaSe chalcogenide plane is sandwiched between two quasihexagonal ( $H$ ) transition metal dichalcogenide (TMD) NbSe<sub>2</sub> layers. LaSe is supposed to be a massive electron donor of NbSe<sub>2</sub> layer(s) [3]. Such a system is the ideal platform to test 2D physics in a bulk compound. Our experimental work as well as calculations [4] have demonstrated that despite being bulk, the single crystal  $(\text{LaSe})_{1.14}(\text{NbSe}_2)_2$  behaves as a doped NbSe<sub>2</sub> monolayer with a rigid doping of 0.55–0.6 electrons per Nb atom. This doping level can be explained by an intuitive chemical model where each LaSe unit transfers one electron to the NbSe<sub>2</sub> layer. As there are two NbSe<sub>2</sub> units per 1.14 LaSe unit, one expects a charge transfer of 0.57 electron per NbSe<sub>2</sub> unit. This is precisely what our previous scanning tunneling microscope (STM) and angle-resolved photoemission

\*Corresponding author: samuely@saske.sk

spectroscopy (ARPES) measurements and density functional theory (DFT) calculations show. Our work thus confirms that Ising superconducting coupling may be a possible scenario for the bulk compound  $(\text{LaSe})_{1.14}(\text{NbSe}_2)_2$ . Notice that until now only monolayer or few-layer systems were found to exhibit Ising superconductivity. Our work suggests that bulk compounds could exhibit it, too.

If we use the same chemical model for  $(\text{LaSe})_{1.14}(\text{NbSe}_2)$  where LaSe layers are simply alternating with  $\text{NbSe}_2$  planes, we find a charge transfer of 1.14 electron per  $\text{NbSe}_2$  unit. However, this is impossible since the undoped  $\text{NbSe}_2$  unit can accept at most one electron. This indicates that the  $\text{NbSe}_2$  band could be completely filled, while the metallicity/superconductivity would reside in LaSe layers. On the other hand, vacancies [5] can reduce the charge transfer, keeping the  $\text{NbSe}_2$  band conducting with much fewer holes than in the case of  $(\text{LaSe})_{1.14}(\text{NbSe}_2)_2$ . A comprehensive study of the superconducting misfit  $(\text{LaSe})_{1.14}(\text{NbSe}_2)_{m=1,2}$  compounds would therefore be of great interest.

The misfit TMDs [6] have a formula  $(MX)_{1+x}(TX_2)_m$  ( $M = \text{Sn, Sb, Pb, Bi, or rare-earth}$ ;  $X = \text{chalcogen}$ ;  $T = \text{transition metal}$ ;  $x$  is a misfit parameter; and  $m = 1, 2, 3$ ) indicating alternating stacking of  $MX$  planes (having NaCl structure, quasiquadratic,  $Q$ ) and TMD layers ( $\text{CdI}_2$  or  $\text{NbS}_2$  structure, quasihexagonal,  $H$ ). Due to different symmetries of the respective layers, misfit results along the crystallographic  $a$  axis. We prepared the misfit layered systems made of LaSe/ $\text{NbSe}_2$  layers, namely  $(\text{LaSe})_{1.14}(\text{NbSe}_2)_2$ , here denoted as  $1Q2H$ , which has the highest transition temperature  $T_c = 5.3$  K [7] among TMD misfits, and  $(\text{LaSe})_{1.14}(\text{NbSe}_2)$ , denoted as  $1Q1H$  with  $T_c$  about 1.3 K [8]. Single crystals were prepared by direct reaction of the La, Nb, and Se elements in stoichiometric ratios as explained elsewhere [7]. The synthesis yielded large black crystals grown on the surface of a black powder. Energy-dispersive x-ray spectroscopy and x-ray diffraction techniques confirmed the expected compositions and cell parameters of the  $1Q1H$  and  $1Q2H$  misfit compounds.

A standard lock-in technique was used to measure the magnetic field dependence of the sample resistance in a four-probe configuration at different fixed temperatures down to 100 mK and in magnetic fields up to 30 T in the Laboratoire National de Champs Magnétiques Intenses in Grenoble. The magnetoresistive transitions were also measured at different angles between the  $ab$  plane of the sample and the applied magnetic field, keeping the current always orthogonal to the field. The angular resolution was better than  $0.2^\circ$  with the  $\theta = 0^\circ$  orientation in the  $ab$  plane defined by the highest value of  $B_{c2}$ . The temperature dependence of the resistance at fixed magnetic fields up to 8 T was measured in a He-3 refrigerator in the Centre of Low Temperature Physics Košice. An ac calorimeter installed in the same He-3 cryostat was used to measure the temperature and field sweeps of the specific heat of the same sample as for the resistive measurements. ac calorimetry [9,10] employs periodically modulated power on the sample and measures the resulting sinusoidal temperature response. In our case, heat is supplied to the sample at a frequency  $\omega \sim$  several Hz by a light-emitting diode via optical fiber. The chromel-constantan thermocouple calibrated in the magnetic field is used to record the temperature oscillations.

Although ac calorimetry is not capable of measuring the absolute values of the heat capacity, it is very sensitive to relative changes in minute samples.

Figure 1(a) shows the structure of the  $1Q1H$  and  $1Q2H$  crystals where quasihexagonal  $\text{NbSe}_2$  and quasiquadratic LaSe layers are stacked. The lattice vectors  $\vec{a}$ ,  $\vec{b}$ , and  $\vec{c}$  are indicated.

In the case of  $1Q1H$ , one has an alternation of LaSe and  $\text{NbSe}_2$  layers bound by ionocovalent bonding (left). Notice that this is not a van der Waals material. The center of Fig. 1(a) shows the structure of the  $1Q2H$  compound; a central slab of LaSe/ $Q$  is sandwiched between two  $\text{NbSe}_2/H$  layers. The  $1Q2H$  trilayer is bound by ionocovalent bonding while the crystal is made by van der Waals stacking of the trilayers. Misfit occurs due to mismatch of the  $\vec{a}_Q$  and  $\vec{a}_H$  vectors of the LaSe and  $\text{NbSe}_2$  sublattices, respectively, as shown on the right.

Figure 1(b) displays the temperature dependence of the resistance  $R$  of both  $1Q1H$  and  $1Q2H$  samples indicating a good metallic conductivity with the residual resistivity ratio  $\text{RRR} = 4.3$  and  $5.5$ , respectively. Both samples reveal a sharp transition to the superconducting state with  $T_c = 1.23$  K and the width of the transition between  $0.1$  and  $0.9R_n$  being  $\Delta T_c = 0.1$  K for  $1Q1H$  and  $T_c = 5.7$  K and  $\Delta T_c = 0.2$  K for the  $1Q2H$  compound.

The resistive transitions from the superconducting to the normal state in an applied magnetic field oriented parallel to the  $c$  axis and parallel to the  $ab$  plane are presented in Figs. 1(c)–1(f) for both compounds. The measured resistances were normalized to the high field values. The transitions are shifted to higher fields and broadened with decreasing temperature. The  $1Q1H$  sample shows the superconducting transitions at the fields parallel to the  $c$  axis below 0.5 T down to 100 mK. On the other hand, for the fields parallel to the  $ab$  plane the onset of the normal state starts at 5 T but the full normal state is achieved only above 18 T at 400 mK. In the case of  $1Q2H$  the transitions at fields parallel to  $c$  direction are below 3 T, while for the in-plane fields the transition starts at 20 T and goes far beyond the 28 T limit of the Bitter magnet in Grenoble pointing at some 50 T at 400 mK. We determined the upper critical magnetic field at 90% of the transition to the normal state ( $0.9R_n$ ) to better estimate the huge extent of the superconducting state in these low  $T_c$  samples. The determination of  $B_{c2}$  at the midpoint of the transition yields qualitatively the same conclusions (see the supplemental material [11]).

To evaluate the temperature dependence of  $B_{c2}$  in more detail, we made the measurements of the temperature dependence of the resistance at a fixed magnetic field in a superconducting coil. The measurements were performed on the  $1Q1H$  sample from the same batch as before in the Bitter coil, and a very good agreement between these two measurements was found. Moreover, on the same piece of the sample we performed specific-heat ( $C$ ) measurements using a very sensitive ac calorimetry [9]. By subtracting the normal-state measurement obtained at 1-T field oriented parallel to the  $c$  axis from the one in the superconducting state, we eliminate contributions from the phonons and from the addenda and obtain a difference of the electronic specific heat  $\Delta C/T$ . In

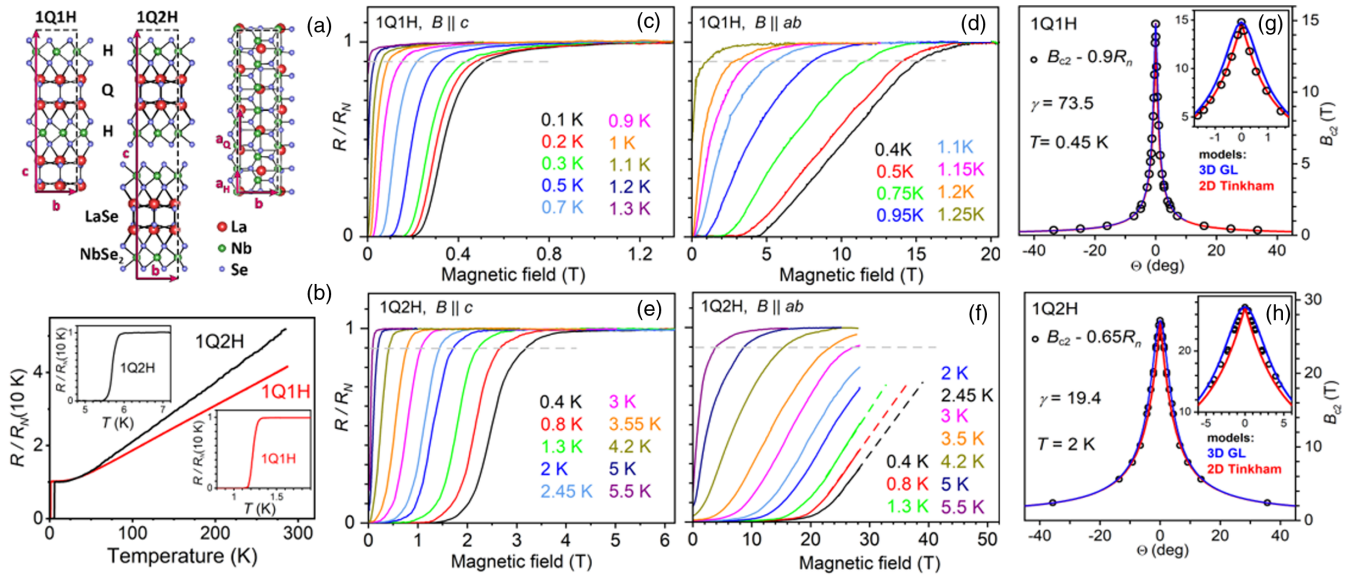


FIG. 1. Crystal structure with lattice vectors represented by red arrows. (a) Left:  $(\text{LaSe})_{1.14}(\text{NbSe}_2)/1\text{Q1H}$ . Center:  $(\text{LaSe})_{1.14}(\text{NbSe}_2)_2 / 1\text{Q2H}$ . In both cases, the unit cell is indicated by a dashed rectangle. Note that trilayer stacks of  $1\text{Q2H}$  are decoupled by van der Waals gap. Right: top view, the dashed rectangle represents a nearly commensurate approximation of the crystal structure with  $4a_Q \approx 7a_H$ . (b) Temperature dependence of resistivity normalized to a residual value for  $1\text{Q2H}$  and  $1\text{Q1H}$ , respectively. The insets show the superconducting transition in detail. (c),(d) Resistive transitions as a function of magnetic field oriented perpendicular (Ref. [8]) and parallel to the  $ab$  plane of the  $1\text{Q1H}$  misfit compound at fixed temperatures, respectively. (e),(f) Resistive transitions for the misfit  $1\text{Q2H}$  for  $B$  perpendicular and parallel with  $ab$  planes of the  $1\text{Q2H}$  system, respectively. Dashed lines in (f) extrapolate resistivity measurements up to fields where linear behavior is expected. Short horizontal dashed lines in (c)–(f) indicate  $R/R_N = 0.9$  and  $0.7$ , respectively. Part (g) shows the angular dependence  $B_{c2}(\theta)$  of the  $1\text{Q1H}$  sample taken at 0.45 K. Part (h) shows the angular dependence  $B_{c2}(\theta)$  of the  $1\text{Q2H}$  sample taken at 2 K.  $B_{c2}(\theta)$  dependences are compared with the anisotropic 3D GL model and the 2D model of Tinkham. Insets display a zoom.

Fig. 2(a) the superconducting transitions are displayed for the indicated fields parallel to the  $c$  axis, while in Fig. 2(b) they are displayed for fields parallel with the  $ab$  plane. One can see that at zero field the superconducting anomaly in specific heat characteristic of the second-order phase transition arises close to the temperature where the resistance sharply drops to zero. For the in-field measurements in both field orientations, the transitions get broadened, but a very good agreement is found between both the superconducting onsets and midpoints of the respective resistive transition and

the specific-heat anomaly. This strongly suggests that both physical quantities are well-characterizing the bulk superconductivity in the system. Remarkably, even if the specific-heat anomaly is well pronounced, the amplitude of the anomaly is quite rapidly suppressed upon increasing magnetic field. This is reminiscent of the situation in high- $T_c$  cuprate superconductors [12,13], where the broadening of the transition in a magnetic field was attributed to the weakening of the coupling between the  $\text{CuO}_2$  planes that limits the superconducting order to two dimensions, thereby enhancing fluctuations.

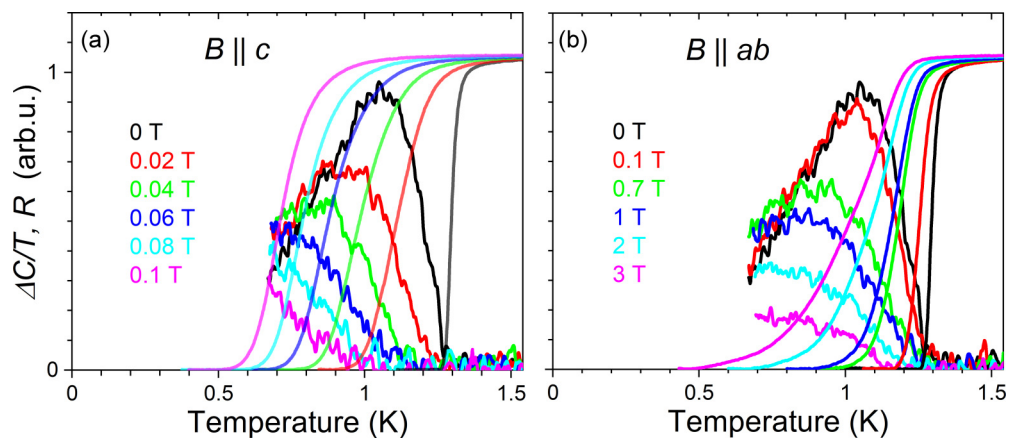


FIG. 2. Superconducting transitions of  $(\text{LaSe})_{1.14}(\text{NbSe}_2)$  obtained by resistive and heat capacity measurements. (a) The superconducting transitions are displayed for the indicated fields parallel to the  $c$  axis, while in (b) they are displayed for the fields parallel with the  $ab$  plane.

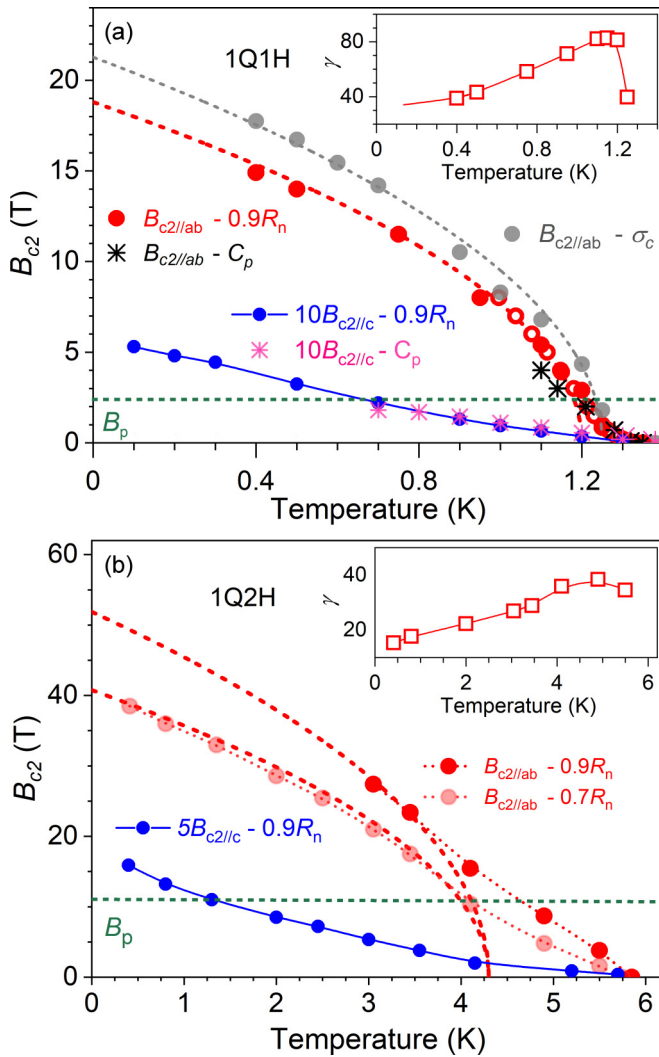


FIG. 3. Upper critical magnetic fields of (a)  $(\text{LaSe})_{1.14}(\text{NbSe}_2)/1\text{Q1H}$  and (b)  $(\text{LaSe})_{1.14}(\text{NbSe}_2)_2/1\text{Q2H}$  misfit compounds; red and blue points show  $B_{c2}$  for fields applied parallel and perpendicular to the  $ab$  planes, respectively, as determined at the 90% of the resistive transition. In (a) solid red points are from field sweeps and open red points are from temperature sweeps of the resistance. Gray points are determined from the interlayer transport, namely from the conductance  $\sigma_c(B) = 1/R_c(B)$  (see the supplemental material [11]). Stars denote values obtained from the onset of the heat-capacity anomaly. Light red points in (b) are taken at  $0.7R_n$ . For better readability,  $B_{c2//c}$  values are multiplied by 10 and 5 for  $1\text{Q1H}$  and  $1\text{Q2H}$ , respectively. Green dashed lines show the Pauli paramagnetic limiting field. In the case of  $1\text{Q2H}$ ,  $B_{c2//ab}$  for fields larger than 30 T are determined at 70% of the resistive transitions. Red and gray dashed lines are approximations by a square-root temperature dependence. Solid and dotted lines are guides for the eye. The temperature dependence of the superconducting anisotropy  $\gamma = B_{c2//ab}/B_{c2//c}$  for both compounds is shown in the insets.

Figure 3 presents the main result of the paper, showing the temperature dependence of upper critical fields for both principal field orientations. Figure 3(a) shows the in-plane  $B_{c2}$  values of  $1\text{Q1H}$  obtained at  $0.9 R_n$  of  $R(B)$  (solid red points) and  $R(T)$  characteristics (open red points). The black aster-

isks are obtained at the onset of the specific-heat anomaly in Fig. 2(b). Below  $T_c$  the resulting  $B_{c2//ab}(T)$  dependence shows a pronounced upturn and changes a curvature from positive to negative. At lower temperatures,  $B_{c2//ab}(T)$  can be well approximated by a square-root temperature dependence (dashed line). The experimental value  $B_{c2//ab}(0.4 \text{ K}) = 15 \text{ T}$  and extrapolated  $B_{c2//ab}(0 \text{ K})$  is close to 19 T. The upper limit of the in-plane upper critical fields is obtained from the interlayer transport, namely from the conductance  $\sigma_c(B) = 1/R_c(B)$  (see the supplemental material [11]) with  $B_{c2//ab}(0 \text{ K})$  above 20 T (gray points and dashed line, approximated square-root temperature dependence). Thus, for fields parallel to the  $ab$  plane of  $1\text{Q1H}$ , all the measurements, namely the specific heat, intralayer (in-plane) resistivity, and interlayer resistivity, provide very consistent results, pointing to an extremely high upper critical field exceeding the Pauli limit  $B_P = 2.2 \text{ T}$  [green dashed line in Fig. 3(a)] by a factor of about 9–10, pointing to a large Zeeman-type spin-orbit interaction. Also, the square-root temperature dependence  $B_{c2//ab}(T)$  is compatible with the spin pair breaking [14]. Contrarily, the orbital pair breaking is naturally present due to a large coherence length in the configuration when the magnetic field is perpendicular to the  $ab$  plane, i.e., in the  $c$  direction. The blue points and the pink asterisks show the temperature dependence of  $B_{c2//c}(T)$  obtained from  $R(B)$  in Fig. 1(c) and from specific heat in Fig. 2(a), respectively.  $B_{c2//c}$  values are multiplied by a factor 10 for clarity. The temperature dependence shows a positive curvature below  $T_c$  changing to a negative one below  $T_c/2$  with extrapolated  $B_{c2//c}(0 \text{ K})$  close to 0.5 T. Then, the superconducting anisotropy  $\gamma = B_{c2//ab}/B_{c2//c}$  at low temperatures reaches about 40.

In Fig. 3(b) the upper critical magnetic fields for  $1\text{Q2H}$  are presented, constructed in a similar way as for  $1\text{Q1H}$ . Here,  $B_{c2//ab}$  established at  $0.9R_n$  (red points) from the resistive transitions is accessible only down to 3 K, where  $B_{c2//ab} = 27.3 \text{ T}$ . Then, we also present the transitions taken at  $0.7R_n$  by the light red points. One can see that below  $T_c = 5.7 \text{ K}$ ,  $B_{c2//ab}(T)$  has a positive curvature changing to a negative one below 4 K. The low-temperature  $B_{c2//ab}(T)$  could be approximated by the square-root temperature dependence providing  $B_{c2//ab}(0 \text{ K})$  equal to 40 and 53 T at 0.7 and  $0.9R_n$ , respectively. This is four to five times higher than the Pauli limit  $B_P = 10.5 \text{ T}$  indicated by the green dashed line. The  $B_{c2//c}(T)$  shown by the blue points (values multiplied by 5 for clarity) reveals a positive curvature all the way down to the lowest temperature of 400 mK. The superconducting anisotropy  $\gamma = B_{c2//ab}/B_{c2//c}$  at low temperatures is approximately 15.

2D superconductivity can also be addressed via studying the angular dependence of the upper critical field  $B_{c2}(\theta)$ , where  $\theta$  is the angle between the applied field and the  $ab$  plane of the sample. Within the anisotropic 3D Ginzburg-Landau (GL) model,  $B_{c2}(\theta)$  can be described by a simple ellipsoidal formula with a rounded maximum around  $\theta = 0$  (magnetic field parallel to the layers),  $(\frac{B_{c2}(\theta)\sin\theta}{B_{c2//c}})^2 + (\frac{B_{c2}(\theta)\cos\theta}{B_{c2//ab}})^2 = 1$ . In the 2D regime, the superconducting layers are decoupled and can be treated as isolated thin films. For this case, Tinkham [15] proposed the equation  $|\frac{B_{c2}(\theta)\sin\theta}{B_{c2//c}}| + (\frac{B_{c2}(\theta)\cos\theta}{B_{c2//ab}})^2 = 1$ , with a finite slope at  $\theta = 0$  making a cusp. This effect was also observed in superconducting superlattices below the

2D-3D transition [16] and also in the case of the extremely anisotropic  $\text{Bi}_{2.2}\text{Sr}_{1.8}\text{CaCu}_2\text{O}_{8+\delta}$  [17].

In Fig. 1(g) we present  $B_{c2}(\theta)$  of the  $1Q1H$  sample taken at 0.45 K. This particular  $1Q1H$  sample has lower perpendicular critical fields  $B_{c2//c}$  than that in Fig. 1(c), probably due to smaller disorder, but it has a very similar  $B_{c2//ab}$ .  $B_{c2}(\theta)$  data are compared with both models: the anisotropic 3D GL and 2D model of Tinkham. For such a high anisotropy ( $\gamma = 73.5$ ), the difference is minor but the inset showing small angles is more compatible with the 2D model, indicating the two-dimensional character of the vortex matter. Figure 1(h) shows the angular dependence  $B_{c2}(\theta)$  for the  $1Q2H$  sample taken at 2 K. Even the inset displaying small angles is not capable of distinguishing the two models since the experimental data lie exactly in between. It is noteworthy that these experiments are rather challenging and  $B_{c2}(\theta)$  with cusplike behavior could be observed only on very tiny samples with a clear plane parallel geometry, while in samples with a slightly wavy surface the angular dependence always revealed the round maximum, probably due to angle averaging.

Lawrence and Doniach [18] described the behavior of layered superconductors in a magnetic field by a model based on stacked two-dimensional superconducting layers coupled together by Josephson tunneling between adjacent planes. In contrast to the isotropic case where the magnetic flux penetration occurs in the form of vortices of circular symmetry, in anisotropic superconductors the vortex cores will be flattened in the interlayer  $c$  direction for fields parallel to the layered structure with  $\xi_c < \xi_{ab}$  for the vortex core radii  $\xi_c$  and  $\xi_{ab}$ , respectively, perpendicular and parallel to the planes. If  $\xi_c$  is bigger than the distance between the adjacent superconducting layers, the system is anisotropic but still three-dimensional, with the upper critical magnetic fields for fields perpendicular and parallel to the layers determined by a product of the corresponding coherence lengths:  $B_{c2//c} = \Phi_0/(2\pi\xi_{ab}^2)$  and  $B_{c2//ab} = \Phi_0/(2\pi\xi_{ab}\xi_c)$ , respectively, where  $\Phi_0$  is the flux quantum. In some cases, including the high- $T_c$  cuprates, the critical fields can be very high, and in extremely anisotropic superconductors  $\xi_c$  could shrink with decreasing temperature below the value of the interlayer distance  $D$ . Then, the vortices become confined between the superconducting layers for parallel fields leading to a dimensional crossover. According to the simplest Lawrence-Doniach model, the parallel upper critical  $B_{c2//ab}$  is predicted to diverge at the temperature  $T^*$ , where  $\xi_c(T^*) = D$ . The real finite value of  $B_{c2//ab}$  is caused by the finite superconducting layer thickness, Pauli paramagnetism, and spin-orbit scattering. Klemm, Luther, and Beasley (KLB) [19] have extended the Lawrence-Doniach model to include these effects. They show that the divergence is removed but the dimensional crossover to a two-dimensional superconductivity is still characterized by a strong upward curvature of  $B_{c2//ab}(T)$ . Experiments on the intercalated layered compounds based on  $2H\text{-TaS}_2$  [20] revealed a strong upward curvature of the temperature dependence of  $B_{c2//ab}$  accompanied by temperature-dependent critical field anisotropy  $\gamma = B_{c2//ab}/B_{c2//c}$  reaching maximum values of about 60 at the dimensional crossover and strong in-plane upper critical fields achieving up to three  $B_P$  on account of the strong spin-orbit scattering rate due to collisions at the interfaces between  $\text{TaS}_2$

layers with the heavy Ta atom ( $Z = 73$ ) and the light organic layers of intercalants.

In both  $(\text{LaSe})_{1.14}(\text{NbSe}_2)$  and  $(\text{LaSe})_{1.14}(\text{NbSe}_2)_2$ , a dimensional crossover is evidenced by an upturn of  $B_{c2//ab}(T)$  and also the temperature-dependent anisotropy factor  $\gamma$  (see the insets in Fig. 3). From  $B_{c2//c}$  data we can estimate the size of the coherence length  $\xi_{ab}$ . For  $1Q1H$  with  $\xi_{ab}(1.2\text{ K}) = 97\text{ nm}$  taking into account the anisotropy factor of about 82 one obtains  $\xi_c(1.2\text{ K}) = 1.2\text{ nm}$ , which is close to the thickness of a stack of one  $H$  and one  $Q$  layer,  $\sim 1.2\text{ nm}$  [21]. Similarly, for  $1Q2H$  at 5 K we obtain  $\xi_{ab} = 40\text{ nm}$  and with  $\gamma \approx 40$  we get  $\xi_c \approx 1\text{ nm}$ . Again, this is close to the distance of about 1.2 nm separating two  $\text{NbSe}_2$  layers across a  $\text{LaSe}$  layer in this compound [7]. Then, the conditions for dimensional transition are fulfilled.

In our previous work [8], we found that the  $(\text{LaSe})_{1.14}(\text{NbSe}_2)$  misfit layer compound behaves as a stack of intrinsic Josephson junctions, making it a 1-K analog to the high- $T_c$   $\text{Bi}_2\text{Sr}_2\text{CaCu}_2\text{O}_{8+\delta}$  superconductor [22]. For this to be the case, the interlayer superconducting coherence length  $\xi_c$  should be shorter than the distance between superconducting atomic layers. In this limit, one can see  $(\text{LaSe})_{1.14}(\text{NbSe}_2)$  misfit as slabs of superconducting layers separated by insulating ones behaving as Josephson tunnel junctions. The short  $\xi_c$  imposes such a high in-plane upper critical magnetic field  $B_{c2//ab} = 1/\xi_c$  for orbital pair breaking that Cooper pairs rather break at the Pauli or Clogston-Chandrasekhar limit  $B_P(T) = 1.84T_c$  (K)  $\approx 2.2\text{ T}$  [23,24] where the Zeeman spin splitting overcomes the superconducting condensation energy. But already preliminary experiments on  $1Q1H$  [25] have shown that  $B_{c2//ab}$  violates the conventional Pauli limit by an enormous factor of 10, almost as high as for the superconductors  $\text{URhGe}$  and  $\text{UCoGe}$  [26], where the ferromagnetic order hinders the Pauli pair breaking mechanism. These findings suggested the presence of an unconventional superconducting state in the  $(\text{LaSe})_{1.14}(\text{NbSe}_2)$  misfit layer, however without a proposed microscopic mechanism to explain the enormous upper critical field.

Such a strong enhancement of the in-plane critical field cannot be explained by the KLB theory taking into account spin-orbit scattering [27]. It would require unrealistically short spin-orbit scattering times given the atomic numbers  $Z = 57$  and 41 for La and Nb, as compared to Ta with  $Z = 73$  [20] as the spin-orbit scattering has been shown to follow the Abrikosov-Gor'kov value  $\sim Z^4$  [28]. Then, different spin-orbit effects must be at play in the case of  $(\text{LaSe})_{1.14}(\text{NbSe}_2)$  and  $(\text{LaSe})_{1.14}(\text{NbSe}_2)_2$ . Our recent paper [4] shows that a single crystal of  $1Q2H$   $(\text{LaSe})_{1.14}(\text{NbSe}_2)_2$ , is electronically equivalent to a  $\text{NbSe}_2$  single atomic layer with an enormous rigid doping of 0.55–0.6 electrons per Nb atom or  $\approx 6 \times 10^{14}\text{ cm}^{-2}$ . An electronic charge transfer occurs from  $\text{LaSe}$  to  $\text{NbSe}_2$  layers. Importantly, also the spin-split Fermi surfaces around  $K$  and  $K'$  points in the Brillouin zone of  $(\text{LaSe})_{1.14}(\text{NbSe}_2)_2$  have been observed in the quasiparticle interference (QPI) data in agreement with DFT calculations, again very similar to the case of the  $\text{NbSe}_2$  monolayer. This is strongly indicating that Ising pairing is responsible for very high in-plane  $B_{c2//ab}$  critical fields despite the fact that it is a fully bulk single crystal.

In the case of the  $1Q1H$   $(\text{LaSe})_{1.14}(\text{NbSe}_2)$  compound, even much larger charge transfer is expected as the electronic donor LaSe is supplying not two NbSe<sub>2</sub> layers but just one. Our preliminary ARPES and STM QPI measurements [29] show a rigid band shift as compared with  $1Q2H$   $(\text{LaSe})_{1.14}(\text{NbSe}_2)_2$ . Further studies are needed to determine whether the NbSe<sub>2</sub> band gets completely filled and what is the real superconducting mechanism in the system.

It is worth noticing that the NbSe<sub>2</sub> surface layer of the  $1Q1H$  crystal is different from the NbSe<sub>2</sub> layers located in the bulk—the surface NbSe<sub>2</sub> layers get only half-doping compared to bulk layers, which are doped from the LaSe layers laying above and underneath the NbSe<sub>2</sub> layer. Then, the electronic structure of this surface layer should be very similar to  $1Q2H$ . Naively, one might speculate that the superconductivity of  $1Q1H$  originates from this topmost layer of NbSe<sub>2</sub> and naturally explain its low  $T_c$ , extreme anisotropy, 2D behavior with cusplike dependence of  $B_{c2}(\theta)$ , and extreme  $B_{c2//ab}$ . However, the specific-heat measurements evidence that these effects are characteristic of the bulk of the sample. Then, in both samples the observed extreme in-plane upper critical fields are bulk effects making our  $(\text{LaSe})_{1.14}(\text{NbSe}_2)_{m=1,2}$  systems very different from the pure NbSe<sub>2</sub>, where the Ising superconductivity is strong only in the case of atomic monolayer, while adding layers rapidly suppresses  $B_{c2//ab}$  due to restoration of the inversion symmetry. While pristine LaSe crystals feature inversion symmetry, in  $1Q1H$  and  $1Q2H$  both constituents, NbSe<sub>2</sub> and LaSe, lack inversion symmetry [7,21]. If we account for the whole crystal, the total symmetry is just  $I1$  due to incommensurability. This together with a small interlayer hopping may be responsible for Ising superconductivity in our bulk systems [30].

More recently, other mechanisms supporting large  $B_{c2//ab}$  strongly exceeding  $B_p$  have been discussed. In atomically thin 2D systems with inversion symmetry preserved, where the aforementioned Ising superconductivity cannot exist, a large  $B_{c2//ab}$  strongly exceeding  $B_p$  has been detected in PdTe<sub>2</sub> [31] and few-layer stanene [32]. A mechanism called Ising II of su-

perconducting pairing between carriers residing in bands with different orbital indices near the  $\Gamma$  point is proposed, where the bands are spin-split without inversion symmetry breaking. Yet another possibility—pairing with the Rashba spin-orbit coupling—was suggested in the case of a crystalline atomic layer of In on the Si surface [33]. The particular mechanism of the extremely high in-plane critical field in  $1Q1H$  remains to be explored in our future studies.

In conclusion, it has been shown that two superconducting misfit layer compounds— $(\text{LaSe})_{1.14}(\text{NbSe}_2)$  and  $(\text{LaSe})_{1.14}(\text{NbSe}_2)_2$ —with  $T_c = 1.23$  and 5.7 K, reveal an extremely high in-plane upper critical field reaching about 20 and 50 T, respectively, which is 10 and 5 times more than the respective Pauli paramagnetic limit. Both compounds also show a 2D-3D crossover below  $T_c$  with an upturn in  $B_{c2//ab}$  temperature dependence, a very high- and temperature-dependent superconducting anisotropy, and a cusp in the angular dependence of  $B_{c2}$  for fields parallel to the layers. In  $1Q2H$   $(\text{LaSe})_{1.14}(\text{NbSe}_2)_2$ , which is composed of weakly van der Waals coupled NbSe<sub>2</sub>-LaSe-NbSe<sub>2</sub> trilayers, the Ising spin-orbit coupling is most probably responsible for a very strong in-plane upper critical field. In  $1Q1H$   $(\text{LaSe})_{1.14}(\text{NbSe}_2)$ , with ionocovalent bonding between LaSe and NbSe<sub>2</sub> slabs, the real mechanism behind the huge  $B_{c2//ab}$  remains to be explored. Despite their possible differences, a common denominator in both misfits is a strong charge transfer from LaSe to NbSe<sub>2</sub> that makes them behave as a stack of almost decoupled superconducting atomic layers with missing inversion symmetry. Further transport, STM QPI, and ARPES experiments and DFT calculations are underway to elucidate superconducting mechanism in the systems.

We thank I. Mazin and M. Gmitra for valuable discussions. This work was supported by the projects APVV-20-0425, VEGA 1/0743/19, VEGA 2/0058/20, EMP-H2020 Project No. 824109, the COST action CA16218 (NanocoHybri), and VA SR ITMS2014+313011W856.

- 
- [1] J. M. Lu, O. Zheliuk, I. Leermakers, N. F. Q. Yuan, U. Zeitler, K. T. Law, and J. T. Ye, Evidence for two-dimensional Ising superconductivity in gated MoS<sub>2</sub>, *Science* **350**, 1353 (2015).
- [2] X. Xi, Z. Wang, W. Zhao, J.-H. H. Park, K. T. Law, H. Berger, L. Forró, J. Shan, and K. F. Mak, Ising pairing in superconducting NbSe<sub>2</sub> atomic layers, *Nat. Phys.* **12**, 139 (2016).
- [3] D. Berner *et al.*,  $(\text{LaSe})_{1.14}(\text{NbSe}_2)_2$ —A metal-insulator quantum well crystal? *J. Phys. Condens. Matter* **9**, 10545 (1997).
- [4] R. T. Leriche *et al.*, Misfit layer compounds: A platform for heavily doped 2D transition metal dichalcogenides, *Adv. Funct. Mater.* **31**, 2007706 (2020).
- [5] A. Meerschaut, Y. Mořlo, L. Cario, A. Lafond, and C. Deudon, Charge transfer in misfit layer chalcogenides,  $[(\text{MX})_n]_{1+x}(\text{TX}_2)_m$ : A key for understanding their stability and properties, *Mol. Cryst. Liq. Cryst. Sci. Technol. Sect. A* **341**, 1 (2000).
- [6] J. Rouxel, A. Meerschaut, and G. A. Wiegers, Chalcogenide misfit layer compounds, *J. Alloys Compd.* **229**, 144 (1995).
- [7] R. Roesky, A. Meerschaut, J. Rouxel, and J. Chen, Structure and electronic transport properties of the misfit layer compound  $(\text{LaSe})_{1.14}(\text{NbSe}_2)_2$ , *LaNb<sub>2</sub>Se<sub>5</sub>*, *Z. Anorg. Allg. Chem.* **619**, 117 (1993).
- [8] P. Szabó, P. Samuely, J. Kařmarćk, A. Jansen, A. Briggs, A. Lafond, and A. Meerschaut, Interlayer Transport in the Highly Anisotropic Misfit-Layer Superconductor  $(\text{LaSe})_{1.14}\text{NbSe}_2$ , *Phys. Rev. Lett.* **86**, 5990 (2001).
- [9] J. Kařmarćk, Z. Pribulová, V. Paľuchová, P. Szabó, P. Husanřková, G. Karapetrov, and P. Samuely, Heat capacity of single-crystal  $\text{Cu}_x\text{TiSe}_2$  superconductors, *Phys. Rev. B* **88**, 020507(R) (2013).
- [10] P. F. Sullivan and G. Seidel, Steady-state, ac-temperature calorimetry, *Phys. Rev.* **173**, 679 (1968).
- [11] See Supplemental Material at <http://link.aps.org/supplemental/10.1103/PhysRevB.104.224507> for more details on experiments and data analysis.
- [12] H. H. Wen, G. Mu, H. Luo, H. Yang, L. Shan, C. Ren, P. Cheng, J. Yan, and L. Fang, Specific-Heat Measurement of a

- Residual Superconducting State in the Normal State of Underdoped  $\text{Bi}_2\text{Sr}_{2-x}\text{La}_x\text{CuO}_{6+\delta}$  Cuprate Superconductors, *Phys. Rev. Lett.* **103**, 067002 (2009).
- [13] N. E. Phillips, R. A. Fisher, and J. E. Gordon, The specific heat of high- $T_c$  superconductors, in *Progress in Low Temperature Physics* (Elsevier, Amsterdam, 1992), Vol. 13, Chap. 5, pp. 267–357.
- [14] Y. Matsuda and H. Shimahara, Fulde-Ferrell-Larkin-Ovchinnikov state in heavy fermion superconductors, *J. Phys. Soc. Jpn.* **76**, 051005 (2007).
- [15] M. Tinkham, *Introduction to Superconductivity*, 2nd ed. (Dover, Mineola, NY, 2004).
- [16] C. S. L. Chun, G. G. Zheng, J. L. Vincent, and I. K. Schuller, Dimensional crossover in superlattice superconductors, *Phys. Rev. B* **29**, 4915 (1984).
- [17] M. J. Naughton, R. C. Yu, P. K. Davies, J. E. Fischer, R. V. Chamberlin, Z. Z. Wang, T. W. Jing, N. P. Ong, and P. M. Chaikin, Orientational anisotropy of the upper critical field in single-crystal  $\text{YBa}_2\text{Cu}_3\text{O}$  and  $\text{Bi}_{2.2}\text{CaSr}_{1.9}\text{Cu}_2\text{O}_{8+x}$ , *Phys. Rev. B* **38**, 9280 (1988).
- [18] W. E. Lawrence and S. Doniach, in *Proceedings of the 12th International Conference on Low Temperature Physics* (Academic Press of Japan, Kyoto, 1971).
- [19] R. A. Klemm, A. Luther, and M. R. Beasley, Theory of the upper critical field in layered superconductors, *Phys. Rev. B* **12**, 877 (1975).
- [20] R. V. Coleman, G. K. Eisman, S. J. Hillenius, A. T. Mitchell, and J. L. Vicent, Dimensional crossover in the superconducting intercalated layer compound  $2\text{H-TaS}_2$ , *Phys. Rev. B* **27**, 125 (1983).
- [21] A. Nader, A. Lafond, A. Briggs, A. Meerschaut, and R. Roesky, Structural characterization and superconductivity in the misfit layer compound  $(\text{LaSe})_{1.14}\text{NbSe}_2$ , *Synth. Met.* **97**, 147 (1998).
- [22] N. Morozov, L. Krusin-Elbaum, T. Shibauchi, L. N. Bulaevskii, M. P. Maley, Y. I. Latyshev, and T. Yamashita, High-Field Quasiparticle Tunneling in  $\text{Bi}_2\text{Sr}_2\text{CaCu}_2\text{O}_{8+\delta}$ : Negative Magnetoresistance in the Superconducting State, *Phys. Rev. Lett.* **84**, 1784 (2000).
- [23] A. M. Clogston, Upper Limit for the Critical Field in Hard Superconductors, *Phys. Rev. Lett.* **9**, 266 (1962).
- [24] B. S. Chandrasekhar, A note on the maximum critical field of high-field superconductors, *Appl. Phys. Lett.* **1**, 7 (1962).
- [25] P. Samuely, P. Szabó, J. Kačmarčík, A. G. M. Jansen, A. Lafond, A. Meerschaut, and A. Briggs, Two-dimensional behavior of the naturally layered superconductor  $(\text{LaSe})_{1.14}(\text{NbSe}_2)$ , *Phys. C: Supercond.* **369**, 61 (2002).
- [26] D. Aoki, K. Ishida, and J. Flouquet, Review of U-based ferromagnetic superconductors: Comparison between  $\text{UGe}_2$ ,  $\text{URhGe}$ , and  $\text{UCoGe}$ , *J. Phys. Soc. Jpn.* **88**, 022001 (2019).
- [27] R. A. Klemm, Pristine and intercalated transition metal dichalcogenide superconductors, *Phys. C: Supercond. Appl.* **514**, 86 (2015).
- [28] R. A. Klemm, Experiments on crystalline layered superconductors and SI multilayers, in *Layered Superconductors* (Oxford University Press, Oxford, 2012), Vol. 1, pp. 245–277.
- [29] O. Šofranko, P. Samuely, P. Szabó, J. Kačmarčík, M. Kuzmiak, T. Cren, L. Cario, S. Sasaki, and T. Samuely (unpublished).
- [30] I. Mazin (private communication).
- [31] Y. Liu *et al.*, Type-II Ising superconductivity and anomalous metallic state in macro-size ambient-stable ultrathin crystalline films, *Nano Lett.* **20**, 5728 (2020).
- [32] J. Falson *et al.*, Type-II Ising pairing in few-layer stanene, *Science* **367**, 1454 (2020).
- [33] S. Yoshizawa, T. Kobayashi, Y. Nakata, K. Yaji, K. Yokota, F. Komori, S. Shin, K. Sakamoto, and T. Uchihashi, Atomic-layer Rashba-type superconductor protected by dynamic spin-momentum locking, *Nat. Commun.* **12**, 1462 (2021).